Spin accumulation in metallic nanoparticles



2007 J. Phys.: Condens. Matter 19 165214

(http://iopscience.iop.org/0953-8984/19/16/165214)

IOP PUBLISHING JOURNAL OF PHYSICS: CONDENSED MATTER

J. Phys.: Condens. Matter **19** (2007) 165214 (19pp) doi:10.1088/0953-8984/19/16/165214

# Spin accumulation in metallic nanoparticles

**F Ernult, K Yakushiji, S Mitani and K Takanashi**

Institute for Materials Research, Tohoku University, Katahira 2-1-1 Aoba-ku Sendai, 980-8577, Japan

E-mail: ernult@imr.tohoku.ac.jp

Received 22 September 2006, in final form 9 January 2007
Published 6 April 2007
Online at stacks.iop.org/JPhysCM/19/165214

**Abstract**

The rapid development of spin electronics has emphasized the importance of spin accumulation to transport properties and spin manipulation for quantum computing. The latter requires sufficiently long spin-relaxation times, that may be achieved in nanometric particles. Spin accumulation is then expected to take place and strongly affect the transport properties of the particles. The main transport phenomena occurring in nanoparticles will be reviewed, as well as their interplay with spin accumulation. Recent experimental results confirming the theoretical predictions will also be presented. They show clear evidence of the enhancement of the spin-relaxation time in nanometric particles and are promising for the development of spin-electronics devices.

(Some figures in this article are in colour only in the electronic version)

## 1. Introduction

Spin accumulation is a phenomenon occurring at interfaces between materials with different spin polarizations and inducing a local non-equilibrium magnetization and spin currents [1]. It makes possible spin injection in various materials [2, 3], may lead to current induced magnetization reversal [4], .... Its mechanism relies on the interfacial boundary conditions, requiring a continuity of the chemical potentials. The Fermi levels of each material then split, leading to a local modification of the spin population in the vicinity of the interface. This modifies the interfacial transport properties and, for example, is of primary importance in giant-magnetoresistance (GMR) experiments performed in current-perpendicular-to-the-plane (CPP) geometry as demonstrated by Valet and Fert [5]. The Fermi level splitting extends to a certain distance given by the spin-diffusion length $\lambda_{SF} = \sqrt{D\tau_{SF}}$, where $D$ is the spin-diffusion constant and $\tau_{SF}$ the spin-relaxation time. In this range, due to the gradient of the Fermi levels, spin currents appear and may be separated from charge current by a clever experimental set-up [2]. In spin-transport experiments, the spin-diffusion length is a crucial parameter since it determines the distance above which spin information is lost.

  

Recently, apart from metal/metal interfaces, spin accumulation was studied at metal/semiconductor interfaces, as it is a crucial parameter for spin injection in semiconductors and the development of semiconductor spin electronics [3]. It was also studied in systems with lateral dimensions smaller than the diffusion length so that the shift of the Fermi level is spatially constant [6, 7]. However, if the lateral dimensions are continuously reduced, charging effects may appear and combine with spin accumulation. These effects are due to the Coulomb interactions between electrons and cannot be neglected as soon as the corresponding energies are larger than the thermal activation $k_B T$ [8, 9]. The interplay of charging effects and spin accumulation gives rise to a great variety of effects and may also be used to perform a direct measurement of the spin-relaxation time in nanometric particles. In this paper, we will review the main results concerning this interplay of charging effects and spin accumulation and present recent experimental results about the measurement of the spin-relaxation time in nanometric metallic particles.

However, before going into the details, we will describe spin-accumulation and charging effects separately.

## 2. Spin accumulation in 2D structures

Spin accumulation was first predicted in 1977 by Aronov [1] and measured for the first time in 1985 by Johnson and Silsbee by using ferromagnetic (FM)/non-magnetic (NM) metallic interfaces [2]. The ratio $\rho^{\mathrm{FM}}_{\uparrow/\downarrow}$ of up and down spin electrons driven from a ferromagnetic material (FM) into a non-magnetic material (NM) differs from the equivalent ratio $\rho^{\mathrm{NM}}_{\uparrow/\downarrow}$ inside the non-magnetic material due to the spin polarization of the FM layer. To accommodate this difference, spins accumulate at the interface. If $\rho^{\mathrm{FM}}_{\uparrow/\downarrow}/\rho^{\mathrm{NM}}_{\uparrow/\downarrow} > 1$, the accumulated electrons have an up spin, while they have a down spin in the opposite inequality. To satisfy the charge neutrality, electrons with opposite spin are depleted. Up and down spins therefore exhibit different chemical potentials. This is a current-driven non-equilibrium phenomenon and the accumulated spins tend to relax as they penetrate further in the non-magnetic material. Accordingly, the difference in the chemical potentials vanishes at a distance $d > \lambda_{\mathrm{SF}}$ from the interface where the up and down spins share the same equilibrium chemical potential again. The exact chemical-potential shift is obtained at the equilibrium between spin injection (i.e. spin source) and spin diffusion (i.e. spin sink). As a consequence of this effect, in addition to the charge current, a spin current is transmitted to the non-magnetic metal. Detection of this spin current is not trivial since it is accompanied by a charge current giving rise to spurious effects. Johnson and Silsbee [2, 10, 11] devised an experimental set-up allowing separation of the spin and charge current in order to measure each of them independently (see figure 1). Spins are injected through a first FM/NM interface (this FM layer is the equivalent of a 'polarizer') and detected through a second NM/FM interface(this FM layer is the equivalent of a 'detector'). If a non-equilibrium magnetization is still present in the vicinity of the second interface, i.e. if the distance between the two FM/NM interfaces is smaller than $\lambda_{\mathrm{SF}}$, then a voltage will be detected between the detector and the NM layer. It should be noted that no charge current flows through the detector. The voltage building at the detector FM/NM interface depends on the relative orientation of the magnetization of the detector compared to that of the polarizer. Therefore, by fixing the magnetization of the polarizer and by varying the direction of the magnetization of the detector layer, the detected voltage varies, thus probing the spin accumulation independently of the charge current. By measuring this voltage change as a function of the distance $L$ between the two ferromagnets, one can extract the value of the spin-diffusion length of the non-magnetic material. Spin accumulation decreases with $L$ and finally vanishes for thicknesses much larger

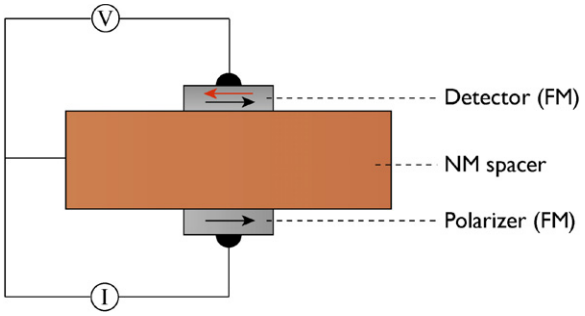


**Figure 1.** Simplified schematic illustration of the experimental set-up used by Johnson and Silsbee to measure spin accumulation in a non-magnetic metallic layer [2].

than the spin-diffusion length $\lambda_{SF}$, so that no voltage change is detected. Knowing $\lambda_{SF}$, the spin-relaxation time $\tau_{SF}$ may then be extracted by using the relation $\lambda_{SF} = \sqrt{D\tau_{SF}}$, where $D$ is the diffusion constant. Unexpectedly long spin-relaxation times were measured in the initial experiments and this result was confirmed by the work of Jedema *et al*, who realized the first measurement of spin accumulation at room temperature [12]. Several works were performed to analyse in detail the experimental results of Johnson, and their results emphasize the influence of the resistance of the FM/NM interfaces on the spin injection efficiency [13–15]. To confirm this prediction experimentally, systems with metallic contacts or with tunnel junctions at the FM/NM interface were studied [16, 17], and indicated an increased efficiency in the case of tunnel barriers. When studying charging effects in nanoparticles, tunnel barriers are a necessity and will in addition help confining the spin accumulation in the nanoparticle.

In the continuation of the works of Johnson and Jedema, several groups studied the effect of spin accumulation in a metallic island [6, 7, 18]. In [6, 7], the lateral dimensions of the non-magnetic island are smaller than the spin-diffusion length and the spin accumulation in the particle is then constant as in the systems used for the study of charging effects detailed in section 3. However, these dimensions are still too large to observe noticeable charging effects at the measurement temperature. In the work of Kimura *et al* [18], the particle is ferromagnetic and the spin accumulation is used to reverse its magnetization. Accumulated spins generate a non-equilibrium magnetization, exerting an exchange interaction on the local magnetic moments. For high enough currents, this interaction may overcome the anisotropy energy and switch the moments of the particle. Due to the non-local configuration, no charge current flows through the particle and only spin current is used to modify the magnetization configuration. This absence of charge currents makes charging effects irrelevant whatever the size of the particle.

## 3. Interplay of charging effects and spin accumulation

Recently, the effects of spin accumulation in 0D systems, i.e. mainly nanoparticles, started to be investigated and have proven useful for the investigation of spin-relaxation time in low-dimensionality environments [19, 20]. In such systems, the lateral dimensions of the particles do not exceed a few nanometres and charging effects now combine with spin accumulation and strongly influence the transport properties. Before presenting the consequences of the interplay of spin-accumulation and charging effects, we will introduce the mechanism of the latter only.

The charging effect arises from the Coulomb interaction between charges, and in particular from the repulsive interactions between electrons. In the simplest case, we consider two neutral

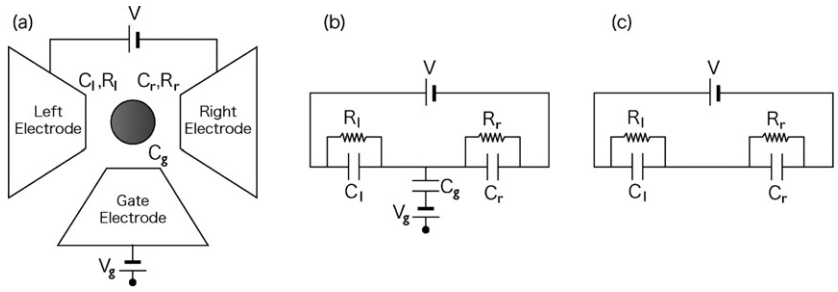


**Figure 2.** Schematic representation and equivalent electric circuit of a double tunnel junction including a nanometric particle. (a) Schematic diagram; (b) equivalent electric circuit including a gate electrode; (c) equivalent electric circuit without gate electrode.

conductive particles separated by a distance $r$. If an electron tunnels from one particle to the other, the total energy of the system rises by about $e^2/r$ due to the creation of an electric dipole. Therefore, only electrons with at least this energy above the Fermi level can be transferred between neutral particles [21, 22]. The energy needed to inject an additional electron in the particle is called the charging energy $E_C$ and its value is related to the intrinsic capacitance $C$ of the particle: $E_C = e^2/C$ [8].

Experimentally, these charging effects are commonly studied in systems in which nanometric particles are separated from electrodes by tunnel barriers, as shown in figure 2(a). The electrodes act as reservoirs from which electrons are injected into the particle (sometimes referred to as the central electrode). The transport is then dominated by the so-called 'single-electron tunnelling' effects, in which electrons tunnel one by one when their energy is high enough to overcome the charging energy of the progressively charged particle. As indicated in figure 2(a), a gate electrode may be added to control the charge stored in the particle and the equivalent electric circuit is shown in figure 2(b). Each tunnel junction is characterized by a resistance $R_i$ and a capacitance $C_i$ and carries a charge $Q_i$, where the subscript $i$ identifies the junction and is denoted l, r or g for the left, right and gate junctions respectively. In such systems in which the particle is sandwiched between two electrodes, the expression of the charging energy becomes $E_C = e^2/2C$ [8]. In the following, to make the explanation simpler, the gate effect will not be considered and the system under consideration is described by the equivalent electrical circuit shown in figure 2(c). To estimate the bias voltage necessary to inject electrons in the particle, it is necessary to calculate the energy change related to the tunnelling of an electron from an electrode to the particle (for example from the left junction to the particle). Prior to this calculation, it is of primary importance to notice that the charging effects will only be noticeable if these energy changes are much larger than the thermal activation $k_B T$. If not, the thermal activation overcomes the charging energy and charging effects become negligible so that tunnelling is allowed at any non-zero bias voltage. This implies a condition on the size of the particles. By approximating the particles by spheres, their self-capacitance is given by $C_{self} = 4\pi\epsilon_0\epsilon_r r$, where $\epsilon_0$ is the permittivity of vacuum, $\epsilon_r$ is the dielectric constant of the tunnel barriers and $r$ the radius of the particle. From an experimental point of view, in order to minimize the spurious effects of thermal fluctuations, the condition $E_C > 10k_B T$ is often used and the maximum diameter suitable for the observation of charging effects is given by

$$d < \frac{e^2}{40\pi\epsilon_0\epsilon_r k_B T}. \tag{1}$$

Table 1 shows the maximum diameter obtained from this expression as a function of temperature for MgO tunnel barriers ($\epsilon_r = 9.8$).

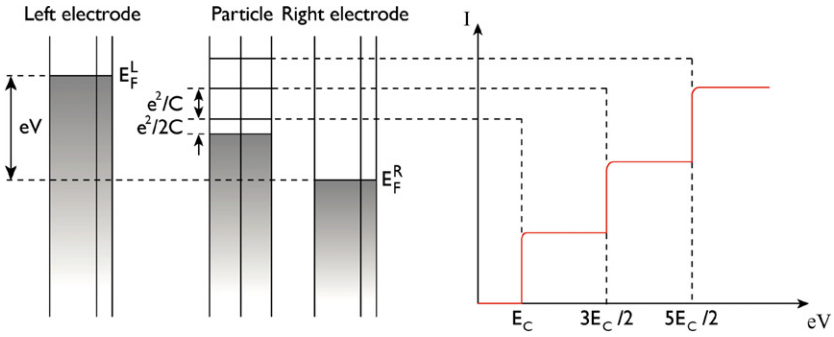


**Figure 3.** Schematic representation of the Coulomb staircase and of the energy levels inside the particle. The levels are split by the charging energy. A step appears in the $I(V)$ characteristic every time the Fermi level of the source (left) electrode matches one of the levels of the particle.

**Table 1.** Maximum diameter for the observation of charging effects.

| Temperature (K) | Maximum diameter (nm) |
|---|---|
| 4.2 | 41 |
| 20 | 8.6 |
| 77 | 2.2 |
| 300 | 0.6 |

In the initial state, we assume that $n$ electrons dwell on the particle. The energy change due to the tunnelling from an electrode to the particle, or inversely, may be simply calculated by expressing the free energy of the system and by using Kirchhoff's law and charge conservation [23].

At very small biases, all these energy changes are positive and tunnelling through the junctions cannot occur since it would lead to an increase of the total energy of the system. The current only starts to flow when the bias voltage reaches a threshold $V_{\text{th}}$ for which one of these energy changes becomes negative. If one supposes that the initial charge state of the particle is $n = 0$, then this threshold is given by

$$V_{\text{th}} = \text{Min}\left\{\frac{e}{2C_l}, \frac{e}{2C_{\text{r}}}\right\}. \tag{2}$$

Similar conditions may be found for the various charge states of the particle, and the $I(V)$ characteristic takes the shape of a staircase known as the Coulomb staircase. The voltage region in which no current flows, i.e. below the first step of the staircase, is referred to as the Coulomb blockade region. The Coulomb staircase may also be understood by drawing the simplified representation of the energy levels of the particle as shown in figure 3. For simplicity, the capacitances of the left and right junctions are supposed equal and denoted by $C_0$. The charging effects then raise the Fermi level by the quantity $e^2/2C_0$ and no tunnelling can occur unless a bias voltage high enough to reach this level is applied. The next steps of the staircase occur when the Fermi level of an electrode matches the level raised above the Fermi level of the particle by $(2n + 1/2)e^2/C_0$.

If ferromagnetic materials are used to prepare the electrodes and/or the particle, the charging effects have also been shown to have strong consequences on the magnetoresistance of the double tunnel junctions [24, 25]. Barnas and Fert [24] assumed a double tunnel junction with both electrodes and the central particle being ferromagnetic. The spin relaxation time

was assumed to be shorter than the time interval between two successive tunnelling events. The spins therefore relax before tunnelling out of the particle and both spin populations share the same Fermi level. Their results indicate that the magnetoresistance of such a double tunnel junction oscillates as a function of the bias voltage, the successive peaks of the TMR corresponding to the steps of the associated Coulomb staircase. Majumdar *et al* [25] found similar results by assuming a variety of configurations including both ferromagnetic and non-magnetic materials. Such an effect has since been observed in various systems including FM particles [26–29]. It was then not long before spin accumulation was taken into account in the models. If the spin-relaxation time becomes larger than the time between two successive tunnelling events, the tunnelling spins do not relax before leaving the particle and start to accumulate [30–35]. In this case, and as described in section 2, the Fermi level of the particles becomes split. However, given the small lateral size of the particle, the splitting is constant in the whole particle. Furthermore, this splitting does not only affect the Fermi level itself, but is passed on the energy levels coming from the charging effects. This will therefore alter the shape of the steps of the Coulomb staircase. This shift, denoted by $\Delta E_{\mathrm{F}}$, is directly related to the current flowing through the system and to the spin-relaxation time $\tau_{\mathrm{SF}}$ by the following expression:

$$I_{\mathrm{r},\sigma} - I_{l,\sigma} = e\frac{D_\sigma \Omega \Delta E_{\mathrm{F}}^{\sigma}}{\tau_{\mathrm{SF}}} \tag{3}$$

where $I_{i,\sigma}$ is the current of electrons with spin $\sigma$ through the $i$th junction, $D_\sigma$ the density of states at the Fermi level for spin $\sigma$ and $\Omega$ the volume of the particle. This expression simply expresses the fact that all the electrons that are not transferred through the particle without spin loss are diffused in the particle with a rate $1/\tau_{\mathrm{SF}}$. In the approximation of an infinite relaxation time, this expression simply becomes $I_{\mathrm{r},\sigma} - I_{l,\sigma} = 0$.

The interplay of single-electron tunnelling and spin accumulation makes the resulting effects difficult to model analytically and numerical simulation is often used. The simplest method is the orthodox theory of sequential tunnelling [24, 25]. In this model, by using the energy changes mentioned above, the transition rates $\Gamma_i^{\pm}(n)$ through both tunnel junctions are calculated as well as the probability $p(n)$ for finding $n$ excess electrons on the particle. The probabilities $p(n)$ are then estimated in the stationary state $\mathrm{d}p(n)/\mathrm{d}t = 0$. From these, the Fermi level shifts are estimated self-consistently in order to fulfil equation (3). The current flowing through the system can then be estimated as a function of the applied bias voltage (and gate voltage as well if a gate is included [36]):

$$I = -e\sum_{n=-\infty}^{\infty} p(n)[\Gamma_1^{+}(n) - \Gamma_1^{-}(n)]. \tag{4}$$

Figure 4 shows the $I(V)$ characteristic, Fermi level shifts and magnetoresistance calculated by this model. For simplicity, we have considered a double tunnel junction consisting of two identical ferromagnetic electrodes and a central non-magnetic particle. The parameters of the calculation are as follows: $R_{l,\downarrow}^{P} = 1$ GΩ, $R_{\mathrm{r},\downarrow}^{P} = 10$ MΩ, $P_l = P_{\mathrm{r}} = 0.35$, $C_l = C_{\mathrm{r}} = 1$ aF, $\tau_{\mathrm{SF}} = \infty$, diameter $d = 2.0$ nm and $T = 4.2$ K. We restricted the calculations to the parallel (P) and antiparallel (AP) magnetic configurations in which the magnetizations of the electrodes make an angle of 0 and $\pi$ respectively. The resistances for the up spin channel and the antiparallel configuration were deduced by using the spin polarization. The magnetization of the left electrode was assumed to be fixed while that of the right electrode was reversed to simulate the effect of an external magnetic field. We define by $N_{\uparrow}^{+}$ and $N_{\downarrow}^{+}$ the number of electrons tunnelling into the particle for spin up and down respectively and by $N_{\uparrow}^{-}$ and $N_{\downarrow}^{-}$ the number of electrons tunnelling out from the particle, as well as the ratios

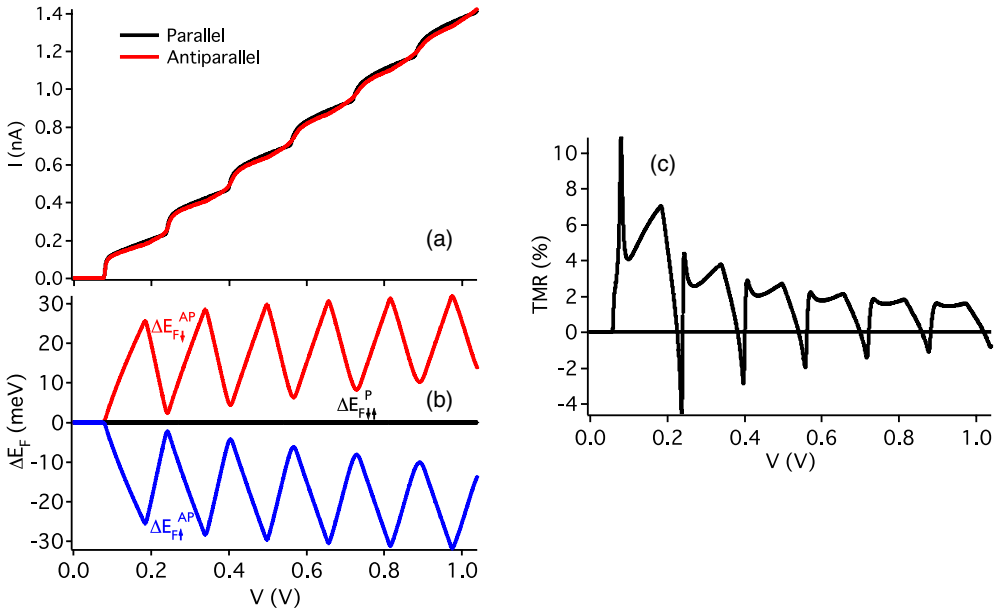


**Figure 4.** (a) Current, (b) Fermi level shifts and (c) TMR of a double tunnel junction with the structure FM/I/NM/I/FM, where I stands for the tunnel barriers. The spin-relaxation time is chosen to be infinite and spin accumulation is manifest as an oscillating shift of the Fermi level.

$\rho^+ = N^+_\uparrow/N^+_\downarrow$ and $\rho^- = N^-_\uparrow/N^-_\downarrow$. Figure 4(a) shows that a Coulomb staircase with the expected period $e/C$ is obtained. Furthermore, in spite of the use of a non-magnetic particle, figure 4(c) shows a non-zero oscillating TMR. Since no spin diffusion takes place in the particle, due to the infinite spin-relaxation time, the electrons retain memory of their initial spin state and contribute to the magnetoresistance. TMR oscillates with a period corresponding to that of the associated Coulomb staircase as predicted by the various models [24, 33]. Secondly, the shift of the Fermi levels also exhibits an oscillatory behaviour with a similar period (see figure 4(b)). However, in the parallel configuration, no spin accumulation occur since the resistances of the two junctions are symmetric and therefore $\rho^+ = \rho^-$. In other words, the number of up electrons tunnelling in the particle is strictly identical to the number of up electrons tunnelling out of the particle, and the same is true for down electrons. Therefore, the Fermi level of the particle does not split since electrons do not accumulate. In the anti-parallel configuration the situation is different since, for example, the number of incoming up electrons is proportional to $D^\uparrow_{\rm elec} D^\uparrow$ while for outgoing up electrons it is $D^\uparrow D^\downarrow_{\rm elec}$, where $D_{\rm elec}$ is the density of states at the Fermi level of the electrodes. This difference leads to non-zero spin accumulation. As shown in figure 4(b), this does not concern the Coulomb blockade area in which the spin accumulation is zero since no electrons flow through the system. Once the Coulomb threshold is overcome, spins start to accumulate and the shift of the Fermi levels shows an oscillatory behaviour with a period corresponding to that of the Coulomb staircase. This oscillation can be simply understood by looking at the configuration of the energy levels (see figure 5). When the threshold is reached (see figure 5(a)), spins start to accumulate (accumulation of up spin and depletion of down spin) and the shift of the Fermi level increases with the bias voltage until the chemical potential of the down spins approaches the value at which a second electron may enter the particle (see figure 5(b)). This second electron is necessarily a down spin and the spin accumulation then decreases. It reaches a minimum at the bias voltage which allows up spin to

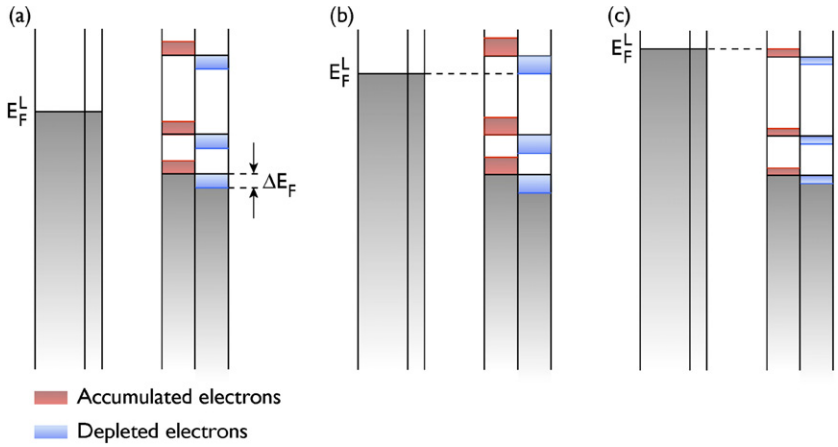


**Figure 5.** Schematic diagram of the energy levels of the left electrode and the central particle. (a) Both up and down spins flow through the first split energy level of the particle and spin accumulation increases; (b) electrons start to flow through the second energy level of the particle. However, only down spins can flow due to the splitting. Spin accumulation then starts to decrease. (c) Up spins are now allowed to flow through the second level of the particle and spin accumulation starts to increase again. This phenomenon will then be repeated for the next levels and give rise to oscillation of the Fermi level shift.

participate in the $n = 2$ state and to accumulate again (see figure 5(c)). This repeats for every step of the Coulomb staircase and therefore leads to the observed oscillations. Furthermore, the sign of TMR changes periodically from positive to negative. Such an effect is not observed in the limit of fast spin relaxation and is therefore a characteristic signature of spin accumulation. It should also be noticed that this sign change is not an intrinsic property of the material of the particle but is only due to the oscillatory behaviour of the Fermi level shift. It is therefore different from previously reported bias-dependent sign changes in single tunnel junctions [70].

As can be seen from equation (3), the shift of the Fermi level, hence the spin accumulation, depends on a number of parameters. Obviously, the first of them is the spin-relaxation time of the electrons dwelling in the particles. For non-infinite spin-relaxation times, a fraction of the spins relax inside the particle and the spin-accumulation effect is reduced. In the case of a double tunnel junction with a non-magnetic particle, TMR decreases as the spin-relaxation time is reduced and tends towards zero for spin-relaxation times shorter than the time interval between two successive tunnelling events, $e/I$ as shown in figure 6. In the case of a ferromagnetic particle, the behaviour of TMR is not that simple, but it appears that the shape of the TMR curve is strongly dependent on the spin-relaxation time. This property may be used to estimate $\tau_{SF}$, as will be shown in section 4.

Apart from the spin-relaxation time, the spin accumulation also appears to depend on the size of the particle via its volume. As a result, the tunnelling magnetoresistance also becomes size dependent. Figure 7 shows the size dependence of the TMR for a system with a non-magnetic particle and the following parameters: $R_l^P = 1\ \mathrm{G\Omega}$, $R_r^P = 10\ \mathrm{M\Omega}$, $P_l = P_r = 0.35$, $\tau_{SF} = 1$ ns, and $T = 4.2$ K. The capacitances are automatically deduced from the mean diameter. For large particles, spin accumulation is almost ineffective and TMR tends towards zero. When the size is decreased, TMR increases as the current density increases and the spin accumulation amplifies.

Finally, the spin accumulation depends on the density of states at the Fermi level. In the case of a non-magnetic particle, only the absolute value of this density matters, but things

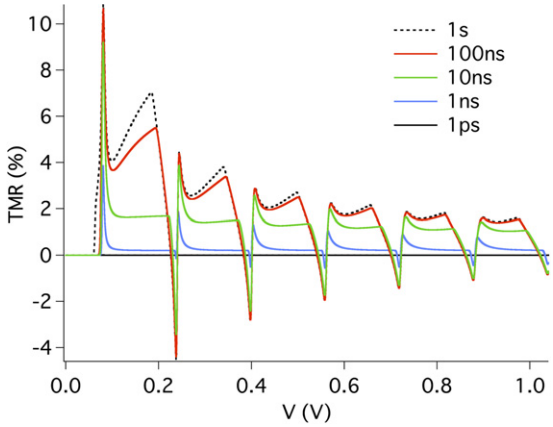


**Figure 6.** Dependence of the TMR ratio on the spin-relaxation time $\tau_{SF}$ in the case of an FM/I/NM/I/FM double tunnel junction with the following parameters: $R_l^P = 1$ GΩ, $R_r^P = 10$ MΩ, $P_l = P_r = 0.35$, and $T = 4.2$ K.

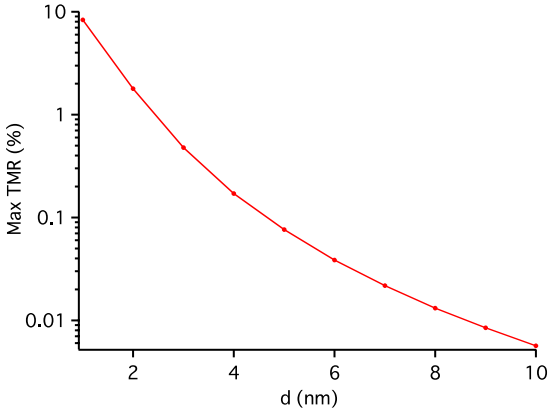


**Figure 7.** Dependence of the TMR ratio on the diameter of the particle in the case of an FM/I/NM/I/FM double tunnel junction with the following parameters: $R_l^P = 1$ GΩ, $R_r^P = 10$ MΩ, $P_l = P_r = 0.35$, $\tau_{SF} = 1$ ns, and $T = 4.2$ K.

are different in the case of a ferromagnetic particle. Barnas and Fert [31] mentioned that the spin accumulation then also depends on the ratio of the density of states for spin up and down, i.e. on the spin polarization of the particle. In order to respect the charge neutrality, the number of accumulated electrons must be equal to the number of depleted electrons and the shifts of the Fermi levels therefore obey $D_\uparrow \Delta E_{F,\uparrow} = D_\downarrow \Delta E_{F,\downarrow}$. The effect of spin accumulation was then predicted to be enhanced when the largest Fermi level shift occurs in the spin channel conducting most of the current. Experimentally, this dependence should be observed by measuring and comparing the spin accumulation in Co and Fe particles. Although the polarizations of the tunnelling electrons of both Co and Fe are quite similar [37, 38], the polarizations of their whole electron populations are quite different: for Fe it is positive (19%), indicating that the majority spins have the highest density of states at the Fermi level, while it is negative (−73%) [39] for cobalt. Figure 8 shows the $I(V)$ characteristics and TMR for particles made of both materials with the following parameters: $R_l^P = 1$ GΩ, $R_r^P = 10$ MΩ,

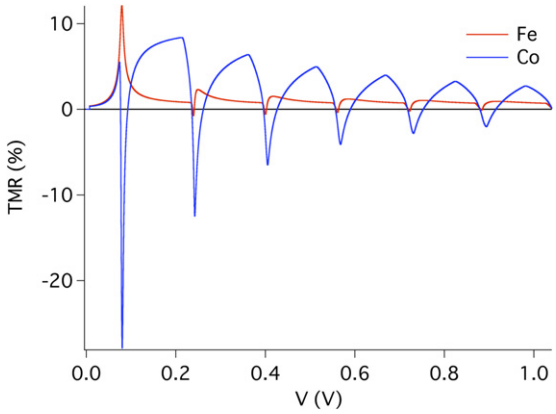


**Figure 8.** Dependence of the TMR ratio on the polarization of the particle in the case of an NM/I/FM/I/FM double tunnel junction. For similar electrodes and magnetic configurations, Co and Fe particles give rise to different TMR curves.

$P_l = 0$ (non-magnetic electrode), $P_r = 0.35$, $C_l = C_r = 1$ aF, $\tau_{SF} = 10$ ns, $d = 4$ nm, and $T = 4.2$ K. Although experimental results in Co particles have been obtained (see section 4) and correlated with the present theory, no result has been reported yet on spin accumulation in Fe particles.

All these dependences may help identify the spin-accumulation effect in nanoparticles in DC current measurements. In addition, Brataas [33–35] *et al* also reported that the AC and transient response of a double tunnel junction exhibit features due to the spin accumulation in the particle. The authors assume that a bias voltage much higher than the Coulomb threshold is suddenly decreased and examine the response of the system until its return to equilibrium. If the final bias voltage is above the Coulomb threshold, they predict that the relaxation of the current will occur with the time constant $RC$. On the other hand, if the final voltage is below the Coulomb threshold, they predict that the relaxation of the current will now occur on a time of the order of the spin-relaxation time, which is usually much longer than $RC$. This is due to the fact that for voltages below the Coulomb threshold the spin of the electrons can only relax in the particle, since the relaxation channels provided by the tunnel junction are blocked. Such a long current relaxation time is an alternative way to identify spin accumulation and estimate the spin-relaxation time in nanoparticles.

Beyond these basic considerations on spin accumulation, several groups studied the interplay of SET and spin accumulation in various configurations and regimes.

### *3.1. Cotunnelling regime*

As mentioned when detailing the results shown in figure 4, spin accumulation vanishes in the Coulomb blockade regime since no current flows through the particle. However, if the resistances of the tunnel junctions become of the order of the quantum resistance $R_K = h/e^2 \approx 25.8$ kΩ, co-tunnelling appears and current may flow below the Coulomb threshold. Co-tunnelling is a high-order tunnelling process in which an electron enters the particle while a second one is leaving the particle simultaneously [40]. The particle then only experiences a virtual charge state and there is no increase of the charging energy in the process. Spin accumulation therefore builds as soon as the voltage is applied and Imamura *et al* [41] showed that it may strongly affect the Coulomb blockade region, hence the onset of sequential

tunnelling, by removing spin-degeneracy. Due to the cotunnelling induced spin accumulation, the threshold above which sequential tunnelling starts now depends on the spin carried by the electron. At first, only electrons with a spin whose Fermi level has been lowered may tunnel into the particle by sequential tunnelling, and only those with a raised Fermi level may tunnel out. The region in which only a given spin population is allowed to enter the particle is called 'half Coulomb blockade' and is given by $-\delta E_F < E_1^{\pm} < \delta E_F$ and $-\delta E_F < E_2^{\pm} < \delta E_F$. In this 'half Coulomb blockade' regime, the authors predict oscillations of the TMR that may be used as a signature of the phenomenon.

More recent works concentrated on these resonances in the 'half Coulomb blockade' [42, 43]. Rather than the orthodox theory of sequential tunnelling, the authors used a more recent model called the 'diagrammatic real-time technique' [44] in order to perform accurate calculations of the current close to these resonances. The main finding is the presence of a clear split peak in the conductance curve at the position of the Coulomb threshold. This splitting is direct evidence of the splitting of the chemical potentials due to spin accumulation. Although this splitting in the conductance peaks could still be observed in pure sequential tunnelling (for the second step and above), the authors emphasize the fact that it appears more clearly in the cotunnelling regime and allows an estimation of the spin-relaxation time.

### *3.2. Energy level quantization*

When the size of the particle becomes small enough, it may be considered as a quantum well, the walls of which correspond to the surrounding tunnel junctions. In this limit, the energy levels of the particle become quantized and additional effects are expected due to the interplay of this quantization with the spin-accumulation and charging effects. In a simple view adopting the free-electron model, the spacing between spin-degenerate energy levels may be written as [45]

$$\delta = \frac{2\pi^2\hbar^2}{mk_F V} \tag{5}$$

where $m$ is the mass of the electron and $k_F$ is the Fermi wavevector. These energy levels appear as conductance peaks every time they are aligned with the Fermi level of the source electrode. However, in order to correctly resolve these levels, the transport measurements must be performed at low enough temperatures satisfying $T < \delta/3.5k_B$. Realistic values for the various parameters of the above mentioned equations give temperatures below a few Kelvin and the experiments aimed at resolving the quantized levels of a metallic particle are often conducted at temperatures of a few hundred millikelvin [45, 46].

The theories previously presented were improved to include this size quantization effect and study in details its influence on the transport properties of double tunnel junctions [47–49]. In addition to the usual Coulomb staircase steps, all these works report an additional fine structure in direct relation to the individual energy levels of the particle. As mentioned above, an additional step is observed in the $I(V)$ characteristics (or peak in the conductance curve) every time the applied bias voltage is in resonance with an energy level of the particle. These fine structures are also observed in the TMR and the shifts of the Fermi levels. They disappear rapidly when the temperature is increased, since the inter-level spacing $\delta$ was chosen to be about an order of magnitude smaller than the charging energy $E_C$ and the related effects are therefore quite sensitive to the thermal activation. Barnas *et al* [32] also discussed additional specific effects due to the size quantization. The authors pointed out that as the gate voltage is varied the period of the observed oscillations is doubled compared to that observed in systems without size quantization. This effect is especially pronounced in the TMR curves and is due to the difference between charge states with even or odd numbers of electrons. This double period

disappears if the temperature is high enough to spontaneously open new spin channels, i.e. if the thermal activation is large enough to overcome the level spacing $\delta$.

Systems in which the inter-level spacing is much higher have also been considered, and the authors of these models assume that only a single level can be accessed by the tunnelling electrons. In this frame, the particle only exhibits four distinct charge states: (a) no electron; (b) one spin-up electron; (c) one spin-down electron; (d) two electrons with opposite spins. The calculations are based on the real-time diagrammatic technique [44] and emphasize the role of spin accumulation [50, 51]. Combined with cotunnelling, it is predicted to give rise to a zero-bias anomaly in the antiparallel configuration [51].

Most of the works presented above focus on parallel and antiparallel configurations in which the magnetizations of the electrodes and particles are collinear. However, interesting phenomena may appear for intermediate angles. Konig *et al* [52] model the transport properties of a non-magnetic particle with a single energy level and discuss the occurrence of a dot–lead interaction similar to an exchange field. When the magnetizations of the electrode are non-collinear, this exchange field exerts a torque on the spin accumulated in the particle and makes it precess, which alters the transport properties.

### *3.3. Current-induced magnetization reversal*

This work on spin precession in nanoparticles suggested the possibility of current-induced magnetization reversal (CIMS) in the particle. This phenomenon is now under intensive study in 2D systems since it may allow a technological leap in the lucrative market of magnetic random-access memory (MRAM) [54]. To briefly introduce the CIMS effect, we consider a simple spin valve. Usually, the directions of the magnetizations of the ferromagnetic electrodes are controlled by an external magnetic field. It is therefore possible to switch from a parallel to an antiparallel configuration. Since the conduction electrons are polarized by the ferromagnetic layers, magnetoresistance effects can then be measured. In 1996, Slonczewski proposed the reversed mechanism, in which the current is polarized by the first FM layer and then exerts a torque on the magnetization of the second FM layer and causes a magnetization reversal [53]. This reversal only occurs if the current is higher than a threshold depending on the saturation magnetization and the thickness of the second FM layer. Readers with a special interest in this field should consult [56] for the detailed basis of the phenomenon. Although the initial proposal stated that this effect would be almost impossible to observe in magnetic junctions due to the high current density required, several groups have succeeded in performing current-induced magnetization switching in $Al_2O_3$ and MgO [57–60] based magnetic tunnel junctions.

The CIMS effect may in fact have two different origins that are still discussed [61]: a torque exerted by the spin of the conduction electrons [53] or a field originating from the spin accumulation taking place at the FM/NM interface [4]. In the case of double tunnel junctions including nanometric particles, the spin torque effect may be inefficient due to the very low current densities caused by the tunnelling barriers. On the other hand, spin accumulation in the particles may be strong enough to affect the transport properties of the system and could be used to switch the magnetization of the particles. In addition to this high spin accumulation, nanoparticles, due to their small lateral dimensions, only count a small number of spins, making their magnetization easy to reverse. Up to now, CIMS has not been observed experimentally in nanoparticles, but several groups have already developed theoretical models. Jalil and Tan [62] extended the orthodox theory to correlate spin accumulation with both current $I$ and magnetization $M$. The authors assumed a ferromagnetic single-domain particle sandwiched between a ferromagnetic source electrode, a non-magnetic drain electrode and a gate. The magnetization of the particle was modelled by a Stoner–Wohlfarth expression in

which the direction of the magnetization is not controlled by an external field, but by the spin accumulation $\Delta S$ in the particle. Spin accumulation was then computed from the orthodox theory to obtain $M(I)$ curves. Numerical calculations in the case of a 15 nm diameter particle indicate that the current density required to switch the magnetization of the particle is of the order of $10^5$ A cm$^{-2}$ and can even be decreased to $3 \times 10^4$ A cm$^{-2}$ if the easy axis of the particle is carefully chosen. These current densities are one order of magnitude smaller than the best results obtained in planar tunnel junctions [58, 59] and are therefore promising for the development of applications. Inoue and Brataas [63] included the discreteness of the energy levels of the particle in their model and also predicted current-induced magnetization reversal in a nanoparticle. They showed that the particle includes both d and s–p-like electrons with different densities of states, and this difference favours a unique direction of the magnetization. Depending on the direction of the current, the magnetization of the particle will preferably remain in its original direction or rotate by $\pi$, unless the anisotropy is too strong.

### *3.4. Multiple particles*

Most of the theoretical work has been used to make predictions for a system including a single particle. However, the models can be easily generalized to a higher number of particles. The particles do not even have to be connected in series, as modelling of an assembly of particles by a simple electrical circuit can be performed [64]. These models are then especially useful for comparison with experiments in which an assembly of particles with distributed characteristics is used [65, 66].

Recently, spin accumulation was included in these generalized models to describe non-magnetic [67] as well as ferromagnetic [68] multi-particle systems. However, the introduction of spin accumulation requires self-consistent calculations to estimate the shift of the Fermi levels in the particles, and for simplicity the models were restricted to double particles only. In the case of ferromagnetic particles, although the shifts of the Fermi levels are somewhat different from those obtained in double tunnel junctions, both $I(V)$ characteristics and TMR are quite similar to the single-particle case. For non-magnetic particles, the authors pointed out that spin accumulation is observed in both parallel and antiparallel configurations even in the case of electrodes made of identical ferromagnetic materials (see section 3 for the single-particle case). This originates from the different spin asymmetries of the conductances of the junctions between the particles and the electrodes and the junction between the two particles. As a result, TMR does not vanish and shows oscillations as a function of the bias voltage, although the electrons have travelled through two successive non-magnetic particles.

## 4. Experimental results

To detect spin accumulation in nanoparticles, we prepared ferromagnetic nanoparticles and measured their transport properties, and in particular TMR since it is strongly dependent on spin accumulation. The particles were made of Co. Due to the negative spin polarization at the Fermi level, the largest shift of the Fermi level occurs for the majority spins, therefore maximizing the influence of spin accumulation on the transport properties (see section 3). The samples were prepared on thermally oxidized Si substrates and the details of the deposition are described elsewhere [19]. The structure of the samples is as follows: Al/Al–O/Al–O–Co/Co/Pt. The top electrode is ferromagnetic while the bottom electrode is non-magnetic Al, and Al–O–Co stands for a so-called granular film made of Co particles randomly distributed in an $AlO_x$ insulating matrix. This makes the hysteresis loop of the samples easier to interpret, since the magnetoresistance is only determined by the relative orientations of the magnetization of the

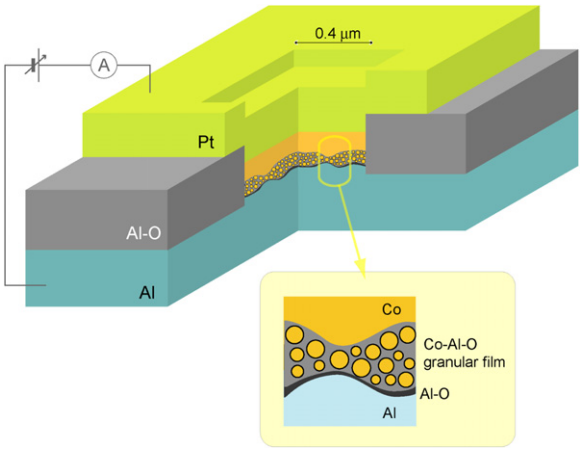


**Figure 9.** Schematic diagram of the micro-fabricated sample with a structure Al/Al–O/Al–O–Co/Co/Pt. The roughness of the bottleneck layer gives rise to area in which a vertical current path includes only one particle [19].

particles and the Co top electrode. In addition, this asymmetry in the magnetic properties of the electrodes leads to spin accumulation in both parallel and anti-parallel configurations. After deposition, the samples were microfabricated into $0.4 \times 0.4\ \mu m^2$ square pillars in order to reduce the number of active particles (see figure 9). The composition of the Al–O–Co granular film was determined to be $Co_{31}Al_{24}O_{45}$ by Rutherford back-scattering, and the average size of the particles was estimated to be 2.5 nm from ZFC–FC curves and transmission electron microscopy observation [69].

The transport properties of the samples were measured at 4.2 K in two different magnetic fields: $H = 0$ and 10 kOe. According to previous experiments [69], $H = 10$ kOe is large enough to saturate the Co particles and the magnetic configuration is then parallel (i.e. the magnetizations of the Co electrode and the particles are parallel). In zero field, the magnetizations of the particles are free to rotate and to align along their respective easy axis. These easy axes being spatially distributed and different for very particle, the zero-field magnetic configuration is therefore not exactly anti-parallel. Due to this possible incomplete AP state, the estimated spin relaxation is a lowest value under which the real spin-relaxation time in the system cannot go (see below). The tunnel magnetoresistance of our samples was defined as $\mathrm{TMR} = (R_{H=0} - R_{H=10\ \mathrm{kOe}})/R_{H=0}$.

Figure 10(a) shows the $I(V)$ characteristics for the different values of the applied field. Coulomb staircase was observed, and is especially marked in the zero-field configuration. In the positive bias region, the steps are observed at the following bias voltages: 15, 50, 85 and 120 mV (and similarly for the negative bias region). The symmetric curve implies a negligible initial background charge on the probed particle. The observation of such a definite Coulomb staircase is usually not expected in samples including a large number of particles. However, in our case, the roughness of the granular film and of the bottleneck layer helps defining restricted current paths containing only a few particles and along which the current preferentially flows (see figure 9). Consequently, only a few particles are probed in parallel.

Due to the different shapes of the $I(V)$ characteristics measured in zero and 10 kOe fields, the two curves periodically cross close to the position of the steps. The corresponding TMR is shown in figure 10(b) and is found to oscillate with the same period as the staircase. Furthermore, it shows a periodic sign change with negative peaks corresponding to the

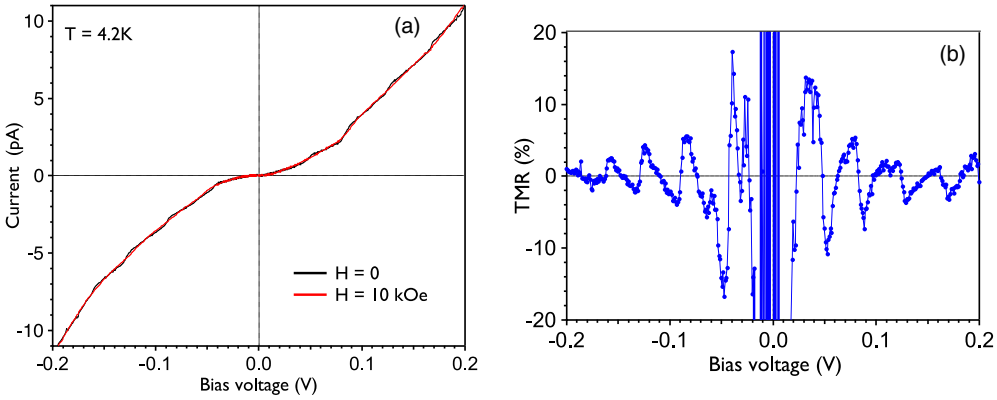


**Figure 10.** $I(V)$ characteristic (a) and TMR (b) of a sample with the structure Al/Al–O/Co–Al–O/Co/Pt. Both Coulomb staircase and TMR oscillations are observed as a function of the applied bias voltage. Periodical sign change of the TMR characteristic of spin accumulation is also observed.

voltages at which the two $I(V)$ characteristics cross each other. The observed TMR is in the range $[-10\%; +15\%]$ and is therefore much higher than the value expected for a similar tunnel junction with continuous central electrode. In the absence of charging effects, the TMR would be $(R_{AP} - R_P)/(R_{AP} + R_{NM})$, where $R_P$ and $R_{AP}$ stand for the resistances of the junction between the particles and the Co top electrode in parallel and anti-parallel configurations respectively, and $R_{NM}$ stands for the resistance of the non-magnetic Co–Al–O/Al–O/Al junction. Given that this junction corresponds to the bottleneck, i.e. the highest resistance, the total TMR is expected to be strongly reduced. If we use the Co polarization deduced from FM/I/SC junctions [38] and the resistance estimated from our measurements, the TMR should not exceed 0.33%. Therefore, even if the measured TMR does not exceed the TMR predicted by Julliere for a single tunnel junction, it appears to be greatly enhanced by the charging effects. Another interesting feature of our results is the periodical sign change of the TMR confirmed by $R(H)$ curves measured at various voltages [19]. Although sign changes of the TMR as a function of the bias voltage have been observed in previous reports for single tunnel junctions [70], no experimental report of periodical change was published.

As mentioned in section 3, periodical sign change of the TMR as a function of the bias voltage is one of the consequences of spin accumulation occurring in nanoparticles. According to the theoretical models, the spin-relaxation time $\tau_{SF}$ in the Co particles exceeds the interval between two successive tunnelling events, estimated to be $t_{dwell} = e/I = 4$ ns at 100 mV. This gives a lower limit of $\tau_{SF}$ but a more precise estimation may be achieved by taking advantage of the strong modification of the shape and intensity of the TMR curve as a function of $\tau_{SF}$ [31, 33, 34]. In particular, when entering the long-spin-relaxation regime, the TMR peaks are predicted to undergo a $\pi$ phase shift.

We performed numerical simulations based on the orthodox theory of sequential tunnelling. In these simulations, we study the case of a single ferromagnetic particle between two electrodes: a ferromagnetic and a non-magnetic one. We restricted the study to the case of collinear magnetizations (i.e. parallel or anti-parallel). As mentioned earlier, it is difficult to estimate experimentally the exact angle between the magnetizations of the particles and the ferromagnetic electrode. However, calculating the TMR between P and AP configurations gives the lower limit of the spin-relaxation time (if the angle in zero field is lower than $\pi$, a longer spin-relaxation time would be needed to recover the amplitude of TMR observed

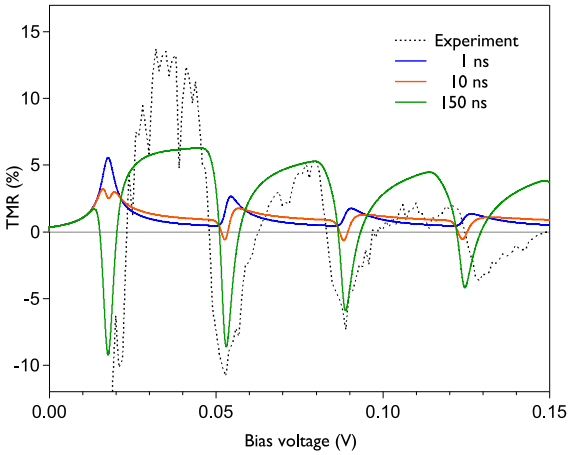


**Figure 11.** Experimentally measured TMR compared with numerical calculations performed for different values of the spin-relaxation time.

experimentally). The capacitances and resistances were estimated from the period and magnitude of the tunnel current respectively. Values are as follows: $C_l = 4.44$ aF, $C_r = 3.00$ aF, $R^P_{l,\uparrow} = 25.0$ GΩ, $R^P_{l,\downarrow} = 51.9$ GΩ, $R^P_{r,\uparrow} = 250$ MΩ and $R^P_{r,\downarrow} = 1.08$ GΩ, $R^{AP}_{l,\uparrow} = R^P_{l,\uparrow}$, $R^{AP}_{l,\downarrow} = R^P_{l,\downarrow}$, $R^{AP}_{r,\uparrow} = R^{AP}_{r,\downarrow} = 519$ MΩ. With these parameters, the polarizations and the temperature (4.2 K) fixed, the last free parameter is the spin-relaxation time in the particle. Figure 11 shows the experimentally measured TMR in positive bias voltage and the curves calculated by applying the orthodox theory for different values of the spin-relaxation time. When the spin relaxation is increased and becomes larger than the interval between successive tunnelling times, the positive peaks located at 18, 53, 88 and 123 mV for $\tau_{SF} = 1$ ns gradually become downwards. In the mean time, the flat regions observed in the fast relaxation limit become upward peaks. The data are best fitted by the curve obtained for $\tau_{SF} = 150$ ns. Such a spin-relaxation time is much larger than the values extracted from CPP-GMR studies [71] and is then quite promising for spin-electronics applications in which the spin of the electrons has to be manipulated.

Similar results were recently obtained in Au particles by Mantel *et al* [20]. In this paper, the structure of the samples is Co/$Al_2O_3$/Au/$Al_2O_3$/Co and the patterning method employed allowed the authors to measure the transport properties of a single particle. Non-zero current was found to flow in the Coulomb blockade area, indicating the presence of co-tunnelling, and spin accumulation was probed by TMR measurements in this co-tunnelling regime. TMR was unambiguously observed and its sign can in no way be attributed to direct tunnelling between the Co electrodes, thus confirming spin accumulation in the Au particle. Although this indicates a rather long spin-relaxation time, no numerical value was presented.

It therefore appears that the spin-relaxation time in both ferromagnetic and non-magnetic materials is greatly enhanced when all lateral dimensions are reduced to a few nanometres. Such a phenomenon was predicted [72] in semiconductor quantum dots and originates from the discretized energy levels due to size quantization. Spin-relaxation times longer than a few microseconds were observed in AlGaAs/GaAs quantum dots [73] and a complete absence of spin decay was even reported in InAs/GaAs quantum dots [74].

In the case of metallic particles several explanations have been advanced to explain the long spin-relaxation time, and as in the semiconductor case they mainly rely on the discretization of

the energy levels. This discreteness leads to a strong reduction of the spin–orbit interaction and therefore suppresses one of the possible spin-relaxation mechanisms [75, 76]. It was in addition mentioned that the spin relaxation is related to the coupling between the atoms of the metallic particles and those of the surrounding insulating matrix [76]. Based on their experimental results on Ag nanoparticles embedded in a $SiO_2$ matrix, Mitrikas *et al* reported that in the case of an amorphous matrix the spin relaxation is further impeded [77]. This is coherent with our results on Co particles since they are embedded in an amorphous $Al_2O_3$ matrix. It was also reported that magnon excitation is suppressed in nanoparticles due to the size quantization of magnon excitations [78].

Finally, Anaya *et al* [79] showed that the spin–orbit interaction is significantly weakened in strongly disordered metals. In their sample, the resistance is lower than the quantum resistance so that no Coulomb blockade is observed due to the occurrence of cotunnelling. The electrons are therefore not confined in a single particle and the quantization of the energy levels cannot be invoked. Their experimental results indicate that the spin–orbit relaxation time is enhanced by at least three orders of magnitude in comparison to weakly disordered metals. To explain this result, they use the Elliot–Yafet relation governing the spin–orbit interaction and adapt it to the case of granular systems. The modified relation shows that the spin–orbit relaxation time is proportional to the inter-granular resistance and should therefore increase with disorder.

## 5. Conclusion

Spin accumulation is a crucial phenomenon in spin transport and may prove invaluable in the case of nanoparticles since the first experimental studies mention greatly enhanced spin-relaxation times in 0D systems. However, further studies are required to unambiguously identify the mechanism leading to this enhancement.

In addition, numerous theoretical studies predicted novel phenomena due to the interplay of charging effects and spin accumulation that still need experimental confirmation, thus making spin accumulation in nanoparticles an exciting research field.

## References

[1] Aronov 1977 *JETP Lett.* **24** 32
[2] Johnson M and Silsbee R H 1985 *Phys. Rev. Lett.* **55** 1790
[3] Schmidt G 2005 *J. Phys. D: Appl. Phys.* **38** R107
[4] Heide C, Zilberman P E and Elliott R J 2001 *Phys. Rev.* B **63** 064424
[5] Valet T and Fert A 1993 *Phys. Rev.* B **48** 7099
[6] Zaffalon M and van Wees B J 2003 *Phys. Rev. Lett.* **91** 186601
[7] Zaffalon M and van Wees B J 2005 *Phys. Rev.* B **71** 125401
[8] Likharev K K 1999 *Proc. IEEE* **87** 606
[9] Grabert H and Devoret M H 1991 *Single Charge Tunnelling* (*NATO ASI Series*)
[10] Johnson M and Silsbee R H 1988 *Phys. Rev.* B **37** 5312
[11] Johnson M 1994 *J. Appl. Phys.* **75** 6714
[12] Jedema F J, Filip A T and van Wees B J 2001 *Nature* **410** 345
[13] Fert A and amd Lee S F 1996 *Phys. Rev.* B **53** 6554
[14] Hershfield S and Zhao H L 1997 *Phys. Rev.* B **56** 3296
[15] Takahashi S and Maekawa S 2003 *Phys. Rev.* B **67** 052409
[16] Jedema F J, Costache M V, Heersche H B, Baselmans J J A and van Wees B J 2002 *Appl. Phys. Lett.* **81** 5162
[17] Ku J H, Chang J, Kim H and Eom J 2006 *Appl. Phys. Lett.* **88** 172510
[18] Kimura T, Otani Y and Hamrle J 2006 *Phys. Rev. Lett.* **96** 037201
[19] Yakushiji K, Ernult F, Imamura H, Yamane K, Mitani S, Takanashi K, Takahashi S, Maekawa S and Fujimori H 2005 *Nat. Mater.* **4** 57
[20] Bernand-Mantel A *et al* 2006 *Appl. Phys. Lett.* **89** 062502

[21] Neugebauer C A and Webb M B 1962 *J. Appl. Phys.* **33** 74
[22] Gorter C J 1951 *Physica* **17** 777
[23] Maekawa S, Takahashi S and Imamura H 2002 *Spin Dependent Transport in Magnetic Nanostructures* ed S Maekawa and T Shinjo (London: Taylor and Francis) p 164
[24] Barnas J and Fert A 1998 *Phys. Rev. Lett.* **80** 1058
[25] Majumdar K and Hershfield S 1998 *Phys. Rev.* B **57** 11521
[26] Nakajima K, Saito Y, Nakamura S and Inomata K 2000 *IEEE Trans. Magn.* **36** 2806
[27] Yakushiji K, Mitani S, Takanashi K and Fujimori H 2002 *J. Appl. Phys.* **91** 7038
[28] Yakushiji K, Mitani S, Takanashi S, Takahashi S, Maekawa S, Imamura H and Fujimori H 2001 *Appl. Phys. Lett.* **78** 515
[29] Ernult F, Yamane K, Mitani S, Yakushiji K, Takanashi K, Takahashi Y K and Hono K 2004 *Appl. Phys. Lett.* **84** 3106
[30] Korotkov A N and Safarov V I 1999 *Phys. Rev.* B **59** 89
[31] Barnas J and Fert A 1998 *Eur. Phys. Lett.* **44** 85
[32] Barnas J and Fert A 1999 *J. Magn. Magn. Mater.* **192** L391
[33] Brataas A, Nazarov Y V, Inoue J and Bauer G E W 1999 *Eur. Phys. J.* B **9** 421
[34] Brataas A, Nazarov Y V, Inoue J and Bauer G E W 1999 *Phys. Rev.* B **59** 93
[35] Brataas A, Nazarov Y V, Inoue J and Bauer G E W 1999 *J. Magn. Magn. Mater.* **198/199** 176
[36] Weymann I and Barnas J 2003 *Phys. Status Solidi* **236** 651
[37] Paraskevopoulos D, Meservey R and Tedrow P M 1977 *Phys. Rev.* B **16** 4907
[38] Meservey R and Tedrow P M 1994 *Phys. Rep.* **238** 173
[39] Kubler J 2000 *Theory of Itinerant Electron Magnetism* (Oxford: Oxford Science Publications) p 235
[40] Averin D V and Odinstov A A 1989 *Phys. Lett.* A **140** 251
[41] Imamura H, Takahashi S and Maekawa S 1999 *Phys. Rev.* B **59** 6017
[42] Martinek J, Barnas J, Maekawa S, Schoeller H and Schon G 2002 *Phys. Rev.* B **66** 014402
[43] Martinek J, Barnas J, Maekawa S, Schoeller H and Schon G 2002 *J. Magn. Magn. Mater.* **240** 143
[44] Schoeller H and Schon G 1994 *Phys. Rev.* B **50** 18436
[45] Ralph D C, Black C T and Tinkham M 1995 *Phys. Rev. Lett.* **74** 3241
[46] Deshmukh M M and Ralph D C 2002 *Phys. Rev. Lett.* **89** 266803
[47] Martinek J, Barnas J, Michalek G, Bulka B R and Fert A 1999 *J. Magn. Magn. Mater.* **207** L1
[48] Barnas J, Martinek J, Michalek G, Bulka B R and Fert A 2000 *Phys. Rev.* B **62** 12363
[49] Brataas A, Hirano M, Inoue J, Nazarov Y V and Bauer G E W 2001 *Japan. J. Appl. Phys.* **40** 2329
[50] Weymann I, Konig J, Martinek J, Barnas J and Schon G 2005 *Phys. Rev.* B **72** 115334
[51] Weymann I, Barnas J, Konig J, Martinek and Schon G 2005 *Phys. Rev.* B **72** 113301
[52] Konig J and Martinek J 2003 *Phys. Rev. Lett.* **90** 166602
[53] Slonczewski J C 1996 *J. Magn. Magn. Mater.* **159** L1
[54] Yagami K, Tulapurkar A A, Fukushima A and Suzuki Y 2005 *J. Appl. Phys.* **97** 10C707
[55] Fontana R E and Hetzler S R 2006 *J. Appl. Phys.* **99** 08N902
[56] Ralph D C and Buhrman R A 2005 *Concepts in Spin Electronics* ed S Maekawa (Oxford: Oxford Science Publications) pp 195–219
[57] Fuchs G D, Emley N C, Krivorotov I N, Braganca P M, Ryan E M, Kiselev S I, Sankey J C, Ralph D C and Buhrman R A 2004 *Appl. Phys. Lett.* **85** 1205
[58] Hayakawa J, Ikeda S, Min Y, Sasaki R, Meguro T, Matsukura F, Takahashi H and Ohno H 2005 *Japan. J. Appl. Phys.* **44** L1267
[59] Kubota H, Fukushima A, Ootani Y, Yuasa S, Ando K, Maehara H, Tsunekawa K, Djayaprawira D D, Watanabe N and Suzuki Y 2005 *Japan. J. Appl. Phys.* **44** L1237
[60] Tulapurkar A A, Suzuki Y, Fukushima A, Kubota H, Maehara H, Tsunekawa K, Djayaprawira D D, Watanabe N and Yuasa S 2005 *Nature* **438** 339
[61] Yang T, Hirohata A, Kimura T and Otani Y 2006 *J. Appl. Phys.* **99** 073708
[62] Jalil M B A and Tan S G 2005 *Phys. Rev.* B **72** 214417
[63] Inoue J and Brataas A 2004 *Phys. Rev.* B **70** 140406
[64] Imamura H, Chiba J, Mitani S, Takanashi K, Takahashi S, Maekawa S and Fujimori H 2000 *Phys. Rev.* B **61** 46
[65] Bar-Sadeh E, Goldstein Y, Zhang C, Deng H, Abeles B and Millo O 1994 *Phys. Rev.* B **50** 8961
[66] Bar-Sadeh E, Goldstein Y, Wolovelsky M, Porath D, Zhang C, Deng H, Abeles B and Millo O 1995 *J. Vac. Sci. Technol.* **13** 1084
[67] Weymann I and Barnas J 2006 *Phys. Status Solidi* **243** 239
[68] Weymann I and Barnas J 2006 *Phys. Rev.* B **73** 033409
[69] Yakushiji K, Mitani S, Takanashi K, Ha J G and Fujimori H 2000 *J. Magn. Magn. Mater.* **212** 75

[70] Tiusan C, Faure-Vincent J, Bellouard C, Hehn M, Jouguelet E and Schuhl A 2004 *Phys. Rev. Lett.* **93** 106602
[71] Bass J and Pratt W Jr 1999 *J. Magn. Magn. Mater.* **200** 274
[72] Khaetskii A V and Nazarov Y V 2000 *Physica* E **6** 470
[73] Fujisawa T, Tokura Y and Hirayama Y 2001 *Phys. Rev.* B **63** 081304
[74] Paillard M, Marie X, Renucci P, Amand T, Jbeli A and Gerard J M 2001 *Phys. Rev. Lett.* **86** 1634
[75] Kawabata A 1970 *J. Phys. Soc. Japan* **29** 902
[76] Khalliulin G G and Khusainov M G 1988 *Sov. Phys.—JETP* **67** 524
[77] Mitrikas G, Trapalis C C and Kordas G 1999 *J. Chem. Phys.* **111** 8098
[78] Yakushiji K, Mitani S, Takanashi K and Fujimori H 1998 *J. Magn. Soc. Japan* **22** 577
[79] Anaya A, Bowman M and Davidovic D 2004 *Phys. Rev. Lett.* **93** 246604